On the eigenvalues optimization of beams with damping patches

VETURIA CHIROIU
Department of Deformable Media
Institute of Solid Mechanics
Ctin Mille 15, P O Box 1-863, Bucharest 010141
ROMANIA
veturiachiroiu@yahoo.com http://www.imsar.ro

Abstract: - The paper discusses the behavior of beams with external nonlocal damping patches made from traditional and auxetic materials. Unlike ordinary local damping models, the nonlocal damping force is modeled as a weighted average of the velocity field over the spatial domain, determined by a kernel function based on distance measures. The performance with respect to eigenvalues is discussed in order to avoid resonance. The optimization is performed by determining the location of patches from maximizing eigenvalues or gap between them.

Key-Words: - eigenvalues, optimization**,** damping patches**,** Euler-Bernoulli beam, nonlocal theory, auxetic material

1 Introduction

The ability of tailoring the best behavior of engineering structures at vibrations consists in a qualitative and quantitative understanding of the damping properties. One way to manipulate the eigenfrequencies of a structure is to vary its damping capacity. Currently, an optimal solution is obtained by maximizing eigenfrequencies or gaps between them, or by minimizing the possibility of internal resonance ordinary local damping models [1]-[5]

In these approaches, studying the damping with the nonlocal theory, will help us understand the mechanisms of damping through the long-range interactions among the particles. The stress at a location is determined by interatomic interactions in the neighbors around that location. The damping force is obtained as a weighted average of the velocity field over the spatial domain, by a kernel function based on distance measures. The deformations at one position produce forces and moments at other points in the structure [6],[7].

The interest in the subject has resulted in a large number of papers which describe nonlocal damping models based on viscoelasticity [8], on the harmonic waves motion in Voigt–Kevin and Maxwell media [9], or on composites with the internal damping torque [10], [11], and so on.

Lei, Friswell and Adhikari [12] have developed a nonlocal damping model including time and spatial hysteresis effects for Euler–Bernoulli beams and Kirchoff plates. The starting point of this theory is the damping force which depends at a given point on the past history of a velocity field over a certain domain, through a kernel function.

In this paper we apply the Lei, Friswell and Adhikari theory to analyze the dynamic characteristics of the Euler-Bernoulli beams with external damping patches made from traditional and auxetic materials. The shear and rotational forces are negligible for this model. The positions of the patches are determined from optimality criteria of maximizing eigenvalues or gap between them in order to avoid resonance. The eigenvalues and optimization problems are solved by the genetic algorithm [13], [14].

2 Problem Formulation

The governing equation of motion for a 1D linear damped continuous dynamic system may be expressed as [12]

$$Lu(x,t) = 0, \quad x \in \Omega, \quad t \in [0,T], \tag{1}$$

where $u(x,t)$ is the displacement vector, x is the spatial variable, t is time, and L is the nonlocal operator defined by

$$Lu(x,t) = \rho(x)\frac{\partial^2}{\partial t^2}u(x,t) + M\frac{\partial}{\partial t}u(x,t),$$

where $\rho(x)$ is the distributed mass density. The operator M is defined as

$$M\frac{\partial}{\partial t}u(x,t) = \int_{\Omega}\int_{0}^{t} C(x,\xi,t-\tau)\frac{\partial}{\partial t}u(\xi,\tau)\mathrm{d}\tau\mathrm{d}\xi, .$$

with $C(x,\xi,t-\tau)$ the kernel function for external damping which is only dependent on the displacement. Eq.(1) is subjected to the initial conditions

$$u(x,0)=u_0(x),\ \frac{\partial}{\partial t}u(x,t)|_{t=0}=v_0(x), \qquad (2a)$$

where $u_0(x)$ and $v_0(x)$ are the initial displacement and velocity. The boundary conditions are given by

$$u(x,t)=\bar{g}_1(x,t) \text{ for } x\in\Gamma_1,$$
$$\frac{\partial}{\partial x}u(x,t)=\bar{g}_2(x,t) \text{ for } x\in\Gamma_2, \qquad (2b)$$

where Γ_1 and Γ_2 are the boundary domains, and $\bar{g}_1(x,t)$ and $\bar{g}_2(x,t)$ are known functions at the boundary. If the damping kernel functions are assumed to be separable in space and time, we can write $C(x,\xi,t-\tau)$ in a general form

$$C(x,\xi,t-\tau)=H(x)c(x-\xi)g(t-\tau). \qquad (3)$$

The expression (3) represents the general form of nonlocal viscoelastic damping model. The function $H(x)$ denotes the presence of nonlocal damping. We have $H(x)=H_0$ (constant) if x is within the patch., and $H(x)=0$ otherwise.

A particular case of (5) is the nonlocal viscous damping (or spatial hysteresis), where the kernel function is given by a delta function in time. In this case, the force depends only on the instantaneous value of the velocity or strain rate $g(t-\tau)=\delta(t-\tau)$, but depends on the spatial distribution of the velocities

$$C(x,\xi,t-\tau)=H(x)c(x-\xi)\delta(t-\tau). \qquad (4)$$

In (4), velocities at different locations within a certain domain can affect the damping force at a given point. This spatial hysteresis that describes the damping mechanism for quasi-isotropic composite beams is similar to the damping model proposed in [15]-[17].

The spatial kernel function, $c(x-\xi)$ is normalized to satisfy the condition $\int_{-\infty}^{\infty}c(x)\mathrm{d}x=1$, and can be choose as an exponential decay or respectively, an error function

$$c(x-\xi)=\frac{\alpha}{2}\exp(-\alpha|x-\xi|),$$
$$c(x-\xi)=\frac{\alpha}{\sqrt{2\pi}}\exp\left(-\frac{1}{2}\alpha^2(x-\xi)^2\right). \qquad (5a)$$

Here α is a characteristic parameter of the damping material. For $\alpha\to\infty$ it results $c(x-\xi)\to 0$. Another form of $c(x-\xi)$ may be taken as the hat respectively, the triangular shapes

$$c(x-\xi)=\frac{1}{l_0} \text{ for } |x-\xi|\le\frac{l_0}{2}, \text{ and 0 otherwise,}$$
$$c(x-\xi)=\frac{1}{l_0}\left(1-\frac{|x-\xi|}{l_0}\right) \text{ for } |x-\xi|\le l_0,$$
$$\text{and 0 otherwise,} \qquad (5b)$$

where l_0 is the influence distance parameter. It results $c(x-\xi)\to 0$ for $|x-\xi|>l_0$. Another form for $c(x-\xi)$ may be the Dirac delta function $\delta(x-\xi)$, which reflects the reacting character of the damping force

$$c(x-\xi)=\delta(x-\xi). \qquad (6)$$

In the case of a reacting damping force (6), there are two cases of $C(x,\xi,t-\tau)$ from (3):

(i) viscoelastic damping (or time hysteresis) with the kernel depending on the past time histories

$$C(x,\xi,t-\tau)=H(x)\delta(x-\xi)g(t-\tau). \qquad (7)$$

(ii) viscous damping with the force depending only on the instantaneous value of the velocity or strain rate

$$C(x,\xi,t-\tau)=H(x)\delta(x-\xi)\delta(t-\tau). \qquad (8)$$

The model (8) represents the well-known viscous damping model. For the kernel function concerned to time $g(t-\tau)$, we consider

$$g(t-\tau)=g_0\mu\exp(-\mu(t-\tau)), \qquad (9)$$

with μ the relaxation constant of the viscoelastic constant for external damping kernel and g_0 a constant.

3 Damped Beam

Consider a beam of length L, in which a number k_p of external nonlocal damping muffled patches of thickness h_p are attached at $(x_1,x_1+\Delta x_1)$, $(x_2,x_2+\Delta x_2)\ldots..(x_k,x_k+\Delta x_k)$, $x_2\ge x_1+\Delta x_1$, $x_i\ge x_{i-1}+\Delta x_{i-1}$, $i=2,...,k$, as shown in Fig. 1.

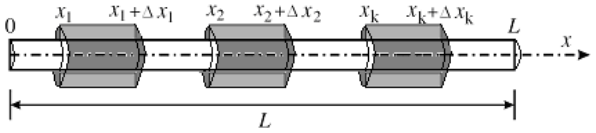

Fig. 1. The beam with nonlocal damping muffled patches.

The design parameters are the number k_p of patches, coordinates x_j, and lengths of patches Δx_j, $j=1,2,...,k_p$, under the conditions $x_2 \geq x_1 + \Delta x_1$, $x_i \geq x_{i-1} + \Delta x_{i-1}$, $i=2,...,k_p$. Since the number of parameters is high, the possible different reduction of the parameter number is versatile. In the forward problem these parameters are known. The equation of motion for the beam is

$$\frac{\partial}{\partial x^2}\left(EI(x)\frac{\partial^2 w(x,t)}{\partial x^2}\right) + \rho A(x)\frac{\partial^2 w(x,t)}{\partial t^2} + \Upsilon = 0, \quad (10)$$

where $EI(x)$ is the bending stiffness (E the Young's modulus of elasticity and $I(x)$ the moment of inertia), $\rho A(x)$ is the mass per unit length (ρ the density and $A(x)$ the cross section area), $w(x,t)$ is the transverse displacement. The third term represents the nonlocal external damping defined over the spatial subdomains $(x_i, x_i + \Delta x_i)$, $i=1,2,...,k$, as

$$\Upsilon = \sum_{i=1}^{k} \int_{x_i}^{x_i+\Delta x_i} \int_{-\infty}^{t} C(x,\xi,t-\tau)\frac{\partial w(\xi,\tau)}{\partial t} \mathrm{d}\tau \mathrm{d}\xi. \quad (11)$$

The damping kernel is defined by (3) with the particular case of the nonlocal viscous damping (or spatial hysteresis), with $C(x,\xi,t-\tau)$ given by (4).

We choose for $c(x-\xi)$ the exponential decay and the error function given by (5a), hat form and the triangular shapes given by (5b) and the Dirac delta function $\delta(x-\xi)$, with both forms for $C(x,\xi,t-\tau)$ namely (7) and (8). The initial conditions (2a) are written as

$$w(x,0) = w_0(x), \quad \frac{\partial}{\partial t} w(x,t)|_{t=0} = v_0(x). \quad (12)$$

The boundary conditions (2b) are written for a clamped beam

$$w(x,t) = 0, \quad \frac{\partial w(x,t)}{\partial x} = 0 \text{ for } x = 0, \ x = L, \quad (13a)$$

for a simple supported beam

$$w(x,t) = 0, \quad \frac{\partial^2 w(x,t)}{\partial x^2} = 0 \text{ for } x = 0, \ x = L, \quad (13b)$$

and for a free end beam

$$\frac{\partial^2 w(x,t)}{\partial x^2} = 0,$$
$$\frac{\partial}{\partial x}\left[EI(x)\frac{\partial^2 w(x,t)}{\partial x^2}\right] = 0 \text{ for } x = 0, \ x = L. \quad (13c)$$

The eigenfrequency problem (10)-(13) is characterised by the integro-differential equation (10), which can be analytically solved by using the cnoidal method [18]-[22].

The general solutions of (10) must be found under the form of a sum of cnoidal functions

$$w(x,t) = \sum_{j=1}^{N} A_j \mathrm{cn}^2(\eta \mid m_j), \ \eta = kx - \omega t + \varphi, \quad (14)$$

where N is the number of cnoidal functions (Jacobian elliptic functions) considered in the series depending on the accuracy required, A_j are unknown constants, k is the wave number, the ω is the frequency and the φ is the phase. M

The Jacobian elliptic function $\mathrm{cn}(\eta \mid m) = \mathrm{cn}\eta$ can be defined with respect to the integral $\eta = \int_0^{\varphi} \frac{\mathrm{d}\theta}{\sqrt{1 - m\sin^2\theta}}$, $0 \leq m \leq 1$, thus $\mathrm{sn}\eta = \sin\varphi$, $\mathrm{cn}\eta = \cos\varphi$, $\mathrm{dn}\eta = \sqrt{1 - m\sin^2\varphi}$.

For $m = 0$ it is obtained $\mathrm{sn}\eta = \sin\eta$, $\mathrm{cn}\eta = \cos\eta$, $\mathrm{dn}\eta = 1$, and for $m = 1$, $\mathrm{sn}\eta = \tanh\eta$, $\mathrm{cn}\eta = \mathrm{sech}\eta$, $\mathrm{dn}\eta = \mathrm{sech}\eta$. By denoting $\eta \mid m_j = \eta_j$ and introducing (14) into (10) we have

$$\frac{\partial}{\partial x^2}\left(EI(x)\frac{\partial^2}{\partial x^2}\left(\sum_{j=1}^{N} A_j \mathrm{cn}^2\eta_j \right)\right) + \rho A(x)\frac{\partial^2}{\partial t^2}\left(\sum_{j=1}^{N} A_j \mathrm{cn}^2\eta_j \right) + \Upsilon = 0, \quad (15)$$

with

$$\Upsilon = \sum_{i=1}^{k} \int_{x_i}^{x_i+\Delta x_i} \int_{-\infty}^{t} C(x,\xi,t-\tau)\frac{\partial}{\partial t}\left(\sum_{j=1}^{N} A_j \mathrm{cn}^2\zeta_j \right) \mathrm{d}\tau \mathrm{d}\xi.,$$
$$\zeta_j = k_j\xi - \omega_j\tau + \varphi_j. \quad (16)$$

The advantage of the cnoidal method consists in the easier mode to choose the constants A_j, $j=1,2,...,N$ by imposing the boundary conditions (3.4) to be satisfied. The eigenvalues are finding by solving the eigenvalue problem (15), (16) with conditions (12), (13).

Let us suppose that the bar is circular with varying diameter $d(x) = d_0\left(2 - a\frac{x}{L}\right) = d_0(2 - bx)$. For $b = 0$ the rod will have a uniform diameter $2d_0$. The area of cross section is $A(x) = \frac{\pi d^2(x)}{4} = A_0(2-bx)^2$, with $A_0 = \frac{\pi d_0^2}{4}$, and

the moment of inertia is $I(x)=\dfrac{\pi d^4(x)}{64}=I_0\left(2-bx\right)^4$ with $I_0=\dfrac{\pi d_0^4}{64}$. The eigenvalue problem is reduced to the equation

$$\sum_{j=1}^{N}(P_j+\rho\omega^2 Q_j+\omega R_j+\Upsilon_j)=0, \qquad (17)$$

where P,Q,R are polynomials in cn, sn and dn, and

$$\Upsilon_j=2\omega A_j\sum_{i=1}^{k}\int_{x_i}^{x_i+\Delta x_i}\int_{-\infty}^{t}C(x,\xi,t-\tau)(\mathrm{cn}\eta_j\mathrm{sn}\eta_j\mathrm{dn}\eta_j)\mathrm{d}\tau\mathrm{d}\xi.$$
$$\eta_j=\eta\,|\,m_j=k\xi-\omega\tau+\varphi.$$

By equating the terms with the same power in cn, sn and dn, a number of K equations are obtained from (17)

$$\lambda_1(A_j,m_j,k,\varphi)=\omega_1,$$
$$\lambda_2(A_j,m_j,k,\varphi)=\omega_2\ldots\ldots, \qquad (18)$$
$$\lambda_K(A_j,m_j,k,\varphi)=\omega_K.$$

The number of unknowns

$$p_M=\{A_j,m_j,k,\varphi,\omega,\ j=1,2...,k_p\},\ M=2k_p+3,$$

is obviously greater than the number of equations $K<M$. A less restrictive approach for the solving of (16) is to form the residuals functions r_K

$$\lambda_l(A_j,m_j,k,\varphi)-\omega_l=r_l,\ l=1,2,...,K.$$

The problem becomes one of minimizing the combined residuals to calculate accurate values for p_M .To solve the eigenvalue problem, a nonlinear least-squares algorithm is proposed.

4 The Inverse Approach

In the formulation of the inverse problem, the bound optimization formulation of Bendsoe, Olhoff and Taylor [23] and Pedersen [2] is used. The unknown parameters are the coordinates x_j and the lengths of patches Δx_j, $j=1,2,...,k_p$, under the conditions $x_2\ge x_1+\Delta x_1,\ x_i\ge x_{i-1}+\Delta x_{i-1},\ i=2,...,k_p$.

We suppose that the number k_p of patches is prescribed. The inverse problem consists in determination of x_j, Δx_j, $j=1,2,...,k_p$, so that all eigenvalues to stay above a given complex constant $C_1+\mathrm{i}C_2$. The formulation of the optimization problem is

Determine x_j, Δx_j, $j=1,2,...,k_p$, *from*:

maximize $|C_1|$, $|C_2|$ *subject to* : *all* $\mathrm{Re}\,|\,\omega|\ge|C_1|$, $\mathrm{Im}\,|\,\omega|\ge|C_2|$

$$\sum_{j=1}^{N}(P_j+\rho\omega^2 Q_j+\omega R_j+\Upsilon_j)=0, \qquad (19)$$

with

$$\Upsilon_j=2\omega A_j\sum_{i=1}^{k}\int_{x_i}^{x_i+\Delta x_i}\int_{-\infty}^{t}C(x,\xi,t-\tau)(\mathrm{cn}\eta_j\mathrm{sn}\eta_j\mathrm{dn}\eta_j)\mathrm{d}\tau\mathrm{d}\xi.$$
$$\eta_j=\eta\,|\,m_j=k\xi-\omega\tau+\varphi.$$

Here, P,Q,R are polynomials in cn, sn and dn.

If we want to maximize the difference between two consecutive eigenvalues, say ω_i and ω_{i+1}, the problem can be formulated as

Determine x_j, Δx_j, $j=1,2,...,k_p$, *from:*

maximize $\mathrm{Re}\,|\,C_4-C_3|$, $\mathrm{Im}\,|\,C_4-C_3|$

subject to : $\mathrm{Re}\,|\,\omega_i|\ge\mathrm{Re}\,|\,C_2|$, $\mathrm{Re}\,|\,\omega_{i+1}|\ge\mathrm{Re}\,|\,C_3|$,
$\mathrm{Im}\,|\,\omega_i|\ge\mathrm{Im}\,|\,C_2|$, $\mathrm{Im}\,|\,\omega_{i+1}|\ge\mathrm{Im}\,|\,C_3|$

$$\sum_{j=1}^{N}(P_j+\rho\omega^2 Q_j+\omega R_j+\Upsilon_j)=0, \qquad (20)$$

with

$$\Upsilon_j=2\omega A_j\sum_{i=1}^{k}\int_{x_i}^{x_i+\Delta x_i}\int_{-\infty}^{t}C(x,\xi,t-\tau)(\mathrm{cn}\eta_j\mathrm{sn}\eta_j\mathrm{dn}\eta_j)\mathrm{d}\tau\mathrm{d}\xi.$$
$$\eta_j=\eta\,|\,m_j=k\xi-\omega\tau+\varphi.$$

5 Beam with patches made from traditional materials

Firstly, we consider that the patches are made from traditional viscoelastic and viscous materials. The first examples 1, 2 and 3 refer to the direct approach in which the coordinates x_j and the lengths of patches Δx_j, $j=1,2,...,k_p$, are known.

Example 1. Let us consider a simply supported aluminum beam of length $L=2$ m, with constant diameter $d=$ 0.005 m, the Young's modulus $E=70\mathrm{GPa}$ and the mass density $\rho=2700\,\mathrm{kg/m^3}$, with a single patch $k_p=1$, $x_1=0.2\mathrm{m}$ and $\Delta x_1=0.2\mathrm{m}$, and thickness $h_p=0.003\mathrm{m}$. Two cases are considered: the nonlocal viscoelastic damping (or time hysteresis) defined by (7) with $\mu=20$ or

$g(t) = 20\exp(-20t)$, and the nonlocal viscous damping defined by (8) with $\mu = \infty$ or $g(t) = \delta(t)$). For each case there are taken four models: (model1) the exponential decay (5a), (M2) the error function (5a), (M3) the hat (5b) and (M4) the triangular shapes (5b). We take $\alpha = 5$ and $l_0 = 0.8$. The number N of cnoidal functions is 4. For $N > 4$ the increase in accuracy of results of the genetic algorithm is not significant.

The three roots of the characteristic equations (17) are determined. These roots can have two distinct forms: (a) one root is real and the other two roots form a complex conjugate pair, or (b) all of the roots are real. The complex conjugate pair of roots in case (a) corresponds to an underdamped oscillator that usually arises when the small damping assumption is made, while the real root corresponds to a purely dissipative motion. Case (b) represents an overdamped system which cannot sustain any oscillatory motion.

Table 1 shows the lower estimates for the first five eigenvalues for the beam with nonlocal viscoelastic damping. Table 2 shows the lower estimates of the first five eigenvalues for the second case of nonlocal viscous damping. It is observed that in both cases, M2 has the largest damping ratios for the first five eigenvalues, while M4 has the smallest damping ratio. All damping models give for each mode, similar imaginary parts.

Table 1. First five eigenvalues for a simply supported beam with one viscoelastic damping patch.

M	Mode 1	Mode 2	Mode 3
1	–4.74 ± 20.15i	–0.26 ± 71.42i	–0.045 ± 160.98i
2	–4.91 ± 20.22i	–0.29 ± 71.66i	–0.051 ± 160.53i
3	–4.75 ± 20.16i	–0.23 ± 71.09i	–0.038 ± 160.51i
4	–4.43 ± 20.39i	–0.15 ± 71.10i	–0.028 ± 160.04i

M	Mode 4	Mode 5
1	–0.017 ± 287.31i	–0.0050 ± 451.67i
2	–0.019 ± 287.76i	–0.0051 ± 451.71i
3	–0.013 ± 287.98i	–0.0012 ± 451.70i
4	–0.008 ± 287.06i	–0.0011 ± 451.74i

Table 2. First five eigenvalues for a simply supported beam with one viscous damping patch.

M	Mode 1	Mode 2	Mode 3
1	–9.97 ± 16.99i	–3.79 ± 72.44i	–3.03 ± 152.66i
2	–10.52 ± 16.94i	–4.28 ± 72.44i	–3.32 ± 152.77i
3	–10.05 ± 16.84i	–3.36 ± 72.48i	–2.51 ± 152.76i
4	–9.12 ± 16.87i	–2.28 ± 72.59i	–1.89 ± 152.58i

M	Mode 4	Mode 5
1	–3.57 ± 283.21i	–2.59 ± 449.03i
2	–4.04 ± 283.23i	–2.64 ± 449.47i
3	–2.73 ± 283.21i	–0.66 ± 449.74i
4	–1.76 ± 283.29i	–0.60 ± 449.82i

Example 2. A simply supported aluminum beam is considered with length $L = 2$ m, with constant diameter $d =$ 0.005m, the Young's modulus $E = 70$ GPa and mass density $\rho = 2700\,\text{kg/m}^3$, with two patches $k_p = 2$ with $x_1 = 0.2$m and $\Delta x_1 = 0.2$m, $x_2 = 1.6$m and $\Delta x_2 = 0.2$m and thickness 0.003m. We $\alpha = 5$ and $l_0 = 0.8$. The table 3 shows the lower estimates of the first five eigenvalues for the beam with nonlocal viscoelastic damping.

Table 4 shows the lower estimates of the first five eigenvalues for the beam for the nonlocal viscous damping. We see that the damping ratios for modes 1 and 2 are greater than those of example 1 for all cases and models. The next modes show increased values of the damping ratios, while the imaginary parts are smaller than those of example 1. The model 2 has the largest damping ratios for the first five eigenvalues, while model 4 has the smallest damping ratio.

Table 3. First five eigenvalues for a simply supported beam with two viscoelastic damping patch.

M	Mode 1	Mode 2	Mode 3
1	–4.82 ± 14.57i	–0.32 ± 63.51i	–0.046 ± 143.56i
2	–4.90 ± 14.99i	–0.39 ± 63.60i	–0.053 ± 143.63i
3	–4.91 ± 14.60i	–0.33 ± 63.32i	–0.039 ± 143.90i
4	–4.65 ± 13.86i	–0.27 ± 63.19i	–0.029 ± 143.42i

M	Mode 4	Mode 5
1	–0.018 ± 280.38i	–0.0052 ± 413.33
2	–0.019 ± 280.42i	–0.0054 ± 413.37
3	–0.015 ± 280.33i	–0.0013 ± 413.11
4	–0.009 ± 280.25i	–0.0012 ± 413.30

Table 4. First five eigenvalues for a simply supported beam with one viscous damping patch.

M	Mode 1	Mode 2	Mode 3
1	–10.07 ± 15.09i	–3.99 ± 70.54i	–3.05 ± 142.46i
2	–10.76 ± 15.22i	–4.77 ± 70.55i	–3.39 ± 142.45i
3	–10.35 ± 15.13i	–3.66 ± 70.68i	–2.57 ± 142.77i
4	–9.40 ± 15.53i	–2.58 ± 70.68i	–1.91 ± 142.78i

M	Mode 4	Mode 5
1	–3.58 ± 270.06i	–2.60 ± 423.03i
2	–4.07 ± 270.00i	–2.65 ± 423.22i
3	–2.75 ± 270.12i	–0.67 ± 423.31i
4	–1.77 ± 270.04i	–0.65 ± 423.30i

Example 3. A cantilever aluminum beam is considered with length $L = 2$ m, with variable diameter $d_0 =$ 0.005 m and $a = 1$, the Young's modulus $E =$ 70 GPa and the mass density $\rho = 2700$ kg/m^3, with a single patch $k = 1$ with $x_1 =$ 0.2m and $\Delta x_1 = 0.2$m, and thickness 0.003m. The table 5 shows the lower estimates of the first five eigenvalues for the cantilever beam with variable

diameter and a nonlocal viscoelastic damping patch. The table 6 shows the lower estimates of the first five eigenvalues for the cantilever beam with variable diameter and a nonlocal viscous damping patch. As compared to results of the example 1, all damping ratios have increased for both cases. The imaginary parts also have increased. It is observed that the model 2 has the largest damping ratios for the first five eigenvalues, while model 4 has the smallest damping ratio.

Table 5. First five eigenvalues for a cantilever beam with variable diameter and viscoelastic damping patch.

M	Mode 1	Mode 2	Mode 3
1	–4.95 ± 25.15i	–0.27 ± 75.44i	–0.047 ± 168.17i
2	–5.02 ± 25.35i	–0.31 ± 75.63i	–0.053 ± 168.33i
3	–4.95 ± 25.52i	–0.25 ± 75.32i	–0.040 ± 168.23i
4	–4.65 ± 24.77i	–0.16 ± 75.10i	–0.031 ± 168.39i

M	Mode 4	Mode 5
1	–0.018 ± 298.44i	–0.0051 ± 466.29i
2	–0.019 ± 298.84i	–0.0053 ± 466.37i
3	–0.014 ± 298.58i	–0.0013 ± 466.47i
4	–0.009 ± 298.33i	–0.0012 ± 466.51i

Table 6. First five eigenvalues for a cantilever beam with variable diameter and viscous damping patch.

M	Mode 1	Mode 2	Mode 3
1	–10.42 ± 17.64i	–3.81 ± 74.60i	–3.18 ± 166.96i
2	–10.97 ± 17.69i	–4.30 ± 74.54i	–3.47 ± 167.17i
3	–10.51 ± 17.59i	–3.38 ± 74.64i	–2.66 ± 167.39i
4	–9.56 ± 18.18i	–2.31 ± 74.75i	–2.04 ± 167.08i

M	Mode 4	Mode 5
1	–3.72 ± 298.71i	–2.66 ± 467.03i
2	–4.19 ± 299.01i	–2.72 ± 467.00i
3	–2.88 ± 299.02i	–0.74 ± 467.24i
4	–1.92 ± 298.79i	–0.50 ± 467.12i

The next step consists in examples 4 and 5 in which the coordinates x_j and the lengths of patches Δx_j, $j = 1,2,...,k_p$, are unknown.

Example 4. Let us consider the example 1, with a single patch $k_p = 1$, of unknown x_1[m], the given length $\Delta x_1 = 0.2$m, and thickness $h_p = 0.003$m. Both cases of nonlocal viscoelastic damping ($\mu = 20$), and of nonlocal viscous damping ($\mu = \infty$) are treated. For each case there is taken the model 1 with $\alpha = 5$ and $l_0 = 0.8$. The number N of cnoidal functions is 4. The inverse problem (19) with

$$C_1 + \mathrm{i}C_2 = -0.005 \pm 451.67\mathrm{i},$$

for the case 1, and

$$C_1 + \mathrm{i}C_2 = -2.59 \pm 449.03\mathrm{i},$$

for the second case is solved by using a genetic algorithm.

The run-time parameters of genetic algorithm are: population size 120, number of generations 60, overall crossover probability 0.9, mutation probability 0.03. The number of iteration for the first case is 496, and for the second case 388. The table 7 gives the estimates for x_1 and the first five eigenvalues of the beam in the first case of nonlocal viscoelastic damping. The table 8 gives the estimates for x_1 and the first five eigenvalues in the second case of nonlocal viscous damping. In both cases, it is maintained the same patch length Δx_1. Modes 3-5 have two estimates for x_1, symmetrically with respect to the ends of beam. By comparing to the similar of the example 1, the damping ratios of all modes are significantly increased. Imaginary parts are greater than those of example 1. In addition, all eigenvalues stay above a given complex constant $C_1 + \mathrm{i}C_2$.

Table 7. Case 1: the location of viscoelastic damping patch (model 1) and the first five eigenvalues for a simply supported beam.

	Mode 1	Mode 2	Mode 3
	–5.87 ± 744.55i	–4.96 ± 1493.49i	–3.24 ± 1873.57i
x_1	1	1	0.46 and 1.34

	Mode 4	Mode 5
	–2.77 ± 2637.39i	–0.52 ± 3553.46i
x_1	0.31 and 1.49	0.22 and 1.58

Table 8. Case 2: the location of viscous damping patch (model 1) and the first five eigenvalues for a simply supported beam

	Mode 1	Mode 2	Mode 3
1	–11.22 ± 715.1i	–6.29 ± 1272.47i	–5.01 ± 1622.66i
x_1	1	1	0.19 and 1.61

	Mode 4	Mode 5
1	–4.37 ± 2290.11i	–3.99 ± 3353.33i
x_1	0.33 and 1.47	0.12 and 1.68

Example 5. Let us consider the example 2, with two patches $k_p = 2$, of unknown x_1[m], x_2[m] the given length $\Delta x_1 = \Delta x_2 = 0.2$m, and thickness $h_p = 0.003$m. Both cases of nonlocal viscoelastic damping ($\mu = 20$), and of nonlocal viscous damping ($\mu = \infty$) are treated. For each case there is taken the model 1 with $\alpha = 5$ and $l_0 = 0.8$. The number N of cnoidal functions is 4. The inverse problem (19) with

$$C_1 + \mathrm{i}C_2 = -0.005 \pm 413.37\mathrm{i},$$

for the case 1, and

$$C_1 + \mathrm{i}C_2 = -2.44 \pm 423.30\mathrm{i},$$

for the second case is solved by using a genetic algorithm. The run-time parameters of genetic algorithm are the same as before. The number of iteration for the first case is 503, and for the second case 481. The table 9 gives the estimates for x_1 and x_2, and the first five eigenvalues of the beam in the first case of nonlocal viscoelastic damping. The table 10 gives the estimates for x_1 and x_2, and the first five eigenvalues in the second case of nonlocal viscous damping. Modes 3-5 have two estimates for x_1 and x_2, symmetrically with respect to the ends of beam. By comparing to the similar of the example 2, the damping ratios of all modes are significantly increased. Imaginary parts are greater than those of example 1. In addition, all eigenvalues stay above a given complex constant $C_1 + \mathrm{i}C_2$.

Table 7. Case 1: the location of the viscoelastic damping patch (model 1) and the first five eigenvalues for a simply supported beam.

	Mode 1	Mode 2	Mode 3
	–5.22 ± 699.32i	–4.93 ± 1292.42i	–3.87 ± 2073.57i
x_1	0.11 nd 1.69	0.18 and 1.62	0.47 and 1.33
x_2	0.21 and 1.59	0.25 and 1.55	0.55 and 1.25

	Mode 4	Mode 5
	–2.59 ± 2537.50i	–2.52 ± 3053.60i
x_1	0.30 and 1.5	0.22 and 1.58
x_2	0.57 and 1.23	0.42 and 1.38

Table 8. Case 2: the location of viscous damping patch (model 1) and the first five eigenvalues for a simply supported beam

	Mode 1	Mode 2	Mode 3
1	–11.22 ± 599.3i	–6.29 ± 1472.47i	–5.01 ± 2222.66i
x_1	0.13 and 1.67	0.31 and 1.49	0.15 and 1.65
x_2	0.20 and 1.6	0.46 and 1.34	0.29 and 1.51

	Mode 4	Mode 5
1	–4.37 ± 2590.11i	–3.99 ± 3386.33i
x_1	0.33 and 1.47	0.12 and 1.68
x_2	0.43 and 1.37	0.32 and 1.48

6 Beam with auxetic paches

Secondly, we consider that the patches are made from auxetic materials. Materials with a negative Poisson ratio ν are auxetic materials. The term *auxetic* is coming from the Greek word *auxetos*, meaning *that which may be increase*. Instead of getting thinner like an elongated elastic band, the auxetic material grows fatter, expanding laterally when stretched. An auxetic system is composed from different materials with different properties with a new mechanical architecture based on tailored properties. For example, the auxetic carbon-fibre reinforced composites or microporous polymers are auxetic systems with various enhancements in the strength and damping properties [26]-[28].

All the major classes of anisotropic materials (polymers, composites, metals, ceramics, honeycomb structures, reticulated metal foams, re-entrant structures, certain rocks and minerals, living bone tissue) can exist in auxetic forms [29]. Plasma crystals are actually observed to have a negative Poisson's ratio, also. Scientists have known about auxetic materials for over a hundred years, though without giving them much a special attention, and treating them as an accident or a curiosity. In an isotropic material the range of Poisson's ratio is from -1.0 to $+0.5$, based on thermodynamic considerations of strain energy in the theory of elasticity. Love [30] presents an example of cubic single crystal pyrite as having a Poisson's ratio of -0.14, and he suggests the effect may result from a twinned crystal.

Typically mechanical properties (for example indentation resistance and shear modulus) are inversely proportional to $(1-\nu^2)$ or $(1+\nu)$. The negative limit of ν for isotropic materials is -1, and $(1-\nu^2)$ or $(1+\nu)$ tend to zero, leading to enhancements in the material properties for auxetic over non-auxetic materials [31]-[33]. The idea is to transform a non-auxetic material into auxetic forms as foams or cellular materials, or to employ techniques to architecture new materials. Two structures made up of auxetic hexagons and spheres are displayed in fig.2.

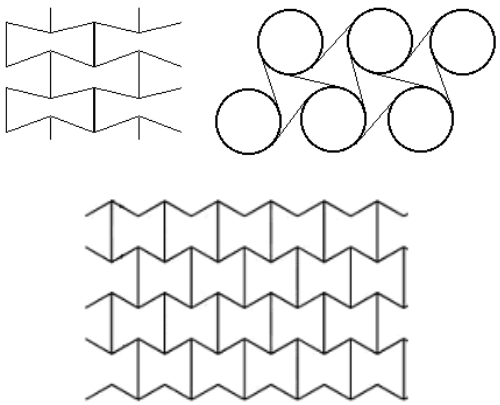

Fig.2. Three structures made up of auxetic hexagons and spheres.

The classical mechanics fails when it is extended to auxetic materials, because these anisotropic materials imply the chiral effects and non-affine deformations [29]. That means, the properties are described by a fifth rank modulus tensor, which changes under an inversion. The source of chirality consists in the existence of a large number of van der Waals contacts and much fewer covalent linkages, which make possible the polymer chain to easily deform to fill any newly created free spaces.

Phenomena associated with chiral elasticity are likely to be of greater interest in materials with auxetic behavior with larger scale structural features. The chirality effects relying upon relatively large scale contribute to the auxetic materials to conform better around corners, and have better pull out resistance and give enhanced impact strength.

The examples 5 and 6 refer to the direct approach in which the coordinates x_j and the lengths of auxetic patches Δx_j, $j=1,2,...,k_p$, are known.

Example 5. Let us consider a simply supported aluminum beam of length $L=2$ m, with constant diameter $d=$ 0.005 m, the Young's modulus $E=70$GPa and the mass density $\rho=2700\,\text{kg/m}^3$, with a single auxetic patch, $k_p=1$ with negative Poisson's ratio $\nu=-0.35$, $\beta=1.5$ and $x_1=0.2$m and $\Delta x_1=0.2$m, and thickness $h_p=0.003$m. The number N of cnoidal functions is 4. For $N>4$ the increase in accuracy of results of the genetic algorithm is not significant. The lower estimates for the first five eigenvalues for the beam are presented in table 9. By comparing to the similar results of example 1, in which the patch is made from a viscoelastic material with positive Poisson's ratio $\nu=0.35$, the damping ratios of all modes are increased.

Table 9. First five eigenvalues for a simply supported beam with one auxetic patch.

M	Mode 1	Mode 2	Mode 3
1	–4.94 ± 20.34i	–0.32 ± 73.56i	–0.051 ± 161.53i
2	–4.98 ± 20.14i	–0.39 ± 73.78i	–0.057 ± 161.51i
3	–4.45 ± 20.10i	–0.23 ± 73.69i	–0.044 ± 161.43i
4	–4.37 ± 20.03i	–0.15 ± 73.44i	–0.031 ± 161.24i

M	Mode 4	Mode 5
1	–0.021 ± 289.76i	–0.0051 ± 455.71i
2	–0.039 ± 289.36i	–0.0054 ± 455.34i
3	–0.023 ± 289.28i	–0.0042 ± 455.27i
4	–0.018 ± 289.11i	–0.0041 ± 455.14i

It is observed that M2 keeps its property to have the largest damping ratios for the first five eigenvalues, while M4 has the smallest damping ratio. All damping models give for each mode, similar imaginary parts.

Example 7. A simply supported aluminum beam is considered with length $L=2$ m, with constant diameter $d=$ 0.005m, the Young's modulus $E=70$ GPa and mass density $\rho=2700\,\text{kg/m}^3$, with two auxetic patches, $k_p=2$ with negative Poisson's ratio $\nu=-0.35$, $\beta=1.5$ with $x_1=0.2$m and $\Delta x_1=0.2$m, $x_2=1.6$m and $\Delta x_2=0.2$m and thickness 0.003m. We $\alpha=5$ and $l_0=0.8$. The table 10 shows the lower estimates of the first five eigenvalues for the beam with nonlocal viscoelastic damping. We see that the damping ratios for all modes are greater than those of example 6. The model 2 has the largest damping ratios for the first five eigenvalues, while model 4 has the smallest damping ratio.

Table 10. First five eigenvalues for a simply supported beam with two auxetic patches.

M	Mode 1	Mode 2	Mode 3
1	–5.12 ± 24.32i	–0.44 ± 75.55i	–0.056 ± 163.34i
2	–5.19 ± 24.79i	–0.47 ± 75.56i	–0.059 ± 163.13i
3	–5.31 ± 24.66i	–0.43 ± 75.02i	–0.053 ± 163.25i
4	–5.05 ± 24.66i	–0.41 ± 75.23i	–0.050 ± 163.72i

M	Mode 4	Mode 5
1	–0.023 ± 292.33i	–0.0055 ± 453.83
2	–0.025 ± 292.40i	–0.0059 ± 453.47
3	–0.021 ± 292.38i	–0.0053 ± 453.15
4	–0.019 ± 292.23i	–0.0051 ± 453.38

The examples 7 and 8 refer to the inverse approach in which the coordinates x_j and the lengths of auxetic patches Δx_j, $j=1,2,...,k_p$, are unknown.

Example 7. Let us consider the example 5, with a single auxetic patch $k_p=1$, of unknown x_1[m], the given length $\Delta x_1=0.2$m, and thickness $h_p=0.003$m. The inverse problem (19) with

$$C_1+\text{i}C_2=-0.0050\pm 466.67\text{i},$$

is solved by using a genetic algorithm. The number of iteration is 487. The estimates for x_1 and the first five eigenvalues are displayed in table 11. By comparing to the similar of the example 5, the damping ratios of all modes are significantly increased. Imaginary parts are greater than those of example 5, all eigenvalues staying above a given complex constant $C_1+\text{i}C_2$.

Table 11. The location of the auxetic patch and the first five eigenvalues for a simply supported beam.

	Mode 1	Mode 2	Mode 3
	–5.87 ± 749.15i	–4.96 ± 1496.29i	–3.24 ± 1873.24i
x_1	1	1	0.43 and 1.57

	Mode 4	Mode 5
	–2.77 ± 2639.31i	–0.52 ± 3558.55i
x_1	0.38 and 1.62	0.27 and 1.73

Example 8. Consider the example 7, with a single auxetic patch $k_p = 1$, of unknown x_1[m], the given length $\Delta x_1 = 0.2$m, and thickness $h_p = 0.003$m. The inverse problem (19) with

$$C_1 + \mathrm{i}C_2 = -0.0050 \pm 466.67\mathrm{i},$$

is solved by using a genetic algorithm. The number of iteration is 509. The estimates for pathes locations and the first five eigenvalues are displayed in table 11. The patches location values are very closed with those obtained in example 5 (see table 8, case 2). By comparing to the similar of the example 7, the damping ratios of all modes are significantly increased. All eigenvalues staying above a given complex constant $C_1 + \mathrm{i}C_2$.

Table 11. The location of the auxetic patches and the first five eigenvalues for a simply supported beam.

	Mode 1	Mode 2	Mode 3
1	–12.32 ± 609.36i	–6.89 ± 1488.42i	–5.71 ± 2243.60i
x_1	0.13 and 1.67	0.31 and 1.49	0.14 and 1.66
x_2	0.20 and 1.6	0.46 and 1.34	0.29 and 1.51

	Mode 4	Mode 5
1	–4.87 ± 2597.42i	–4.19 ± 3377.33i
x_1	0.34 and 1.46	0.12 and 1.68
x_2	0.43 and 1.37	0.32 and 1.48

7 Conclusions

In this paper, the bending of Euler-Bernoulli beams with external nonlocal damping patches is studied. The nonlocal damping force is modeled as a weighted average of the velocity field over the spatial domain, determined by a kernel function based on distance measures.

A simply supported aluminum beam with a single nonlocal damping patch is analyzed for the nonlocal viscoelastic damping (or time hysteresis) defined by (7) with $\mu = 20$ or $g(t) = 20\exp(-20t)$, and for the nonlocal viscous damping defined by (8) with $\mu = \infty$ or $g(t) = \delta(t)$). There are taken four models: (M1) the exponential decay (5a), (M2) the error function (5a), (M3) the hat (5b) and (M4) the triangular shapes (5b);

The lower estimates for the first five eigenvalues are given. In all cases, M2 has the largest damping ratios for the first five eigenvalues, while M4 has the smallest damping ratio. The performance with respect to eigenvalues is discussed next in order to avoid resonance.

The optimization is performed by determining the location of patches from maximizing eigenvalues or gap between them. The formulation of the optimization problem (19) of maximizing eigenvalues is implemented on the example of a simply supported aluminum beam with a single and two patches of unknown locations.

The unknown locations are determined and also the first five eigenvalues for the beam in the first case of viscoelastic damping and in the second case of viscous damping. In both cases,the same patch length is mainteined. Two estimates for the patch location are obtained, symmetrically with respect to the ends of beam. By comparing to the similar non-optimized examples, the damping ratios of all modes are significantly increased. In addition, all eigenvalues stay above a given complex constant.

The paper also presents some remarks regarding the behavior of beams with external auxetic patches. The optimization is performed by determining the location of auxetic patches from maximizing eigenvalues.

The study of bars with auxetic patches is twofold: it promises to make more understandable the damping properties of auxetic patches. On the other hand, it provides the fundaments for construction of new materials with tailored properties, with improved control of damping properties, opening the door to new applications. Negative Poisson's ratio materials easily undergo volume changes but resist shape changes and may thus be viewed as the opposite of rubbery materials, or antirubbers.

Acknowledgements. Supports for this work by the CEEX postdoctoral grant 1531/2006 and the PNII-Idei grant 106/2007 code 247/2007 are gratefully acknowledged.

References:

[1] Abrete, S., Optimal design of laminated plates and shells, *Composite structures*, Vol.29, 1994, pp.269-286.

[2] Pedersen, N.L., *On simultaneous shape and orientational design for eigenfrequency optimisation*, Danish Center for Applied

Mathematics and Mechanics, report nr. 714, June 2006.
[3] Pedersen, N.L., Designing plates for minimum internal resonance, *Struct. Multidisc. Optim*., Vol.28, No.1, 2004, pp.1-10.
[4] Pedersen, N.L., Optimization of holes in plates for control of eigenfrequencies, *Struct. Multidisc. Optim*., Vol.30, No.4, 2005, pp.297-307.
[5]
[6]Eringen, A.C., Edelen, D.G.B., Nonlocal elasticity, *International Journal of Engineering Science*, Vol.10, No.3, 1972, pp.233–248.
[7] Polizzotto, C., Non-local elasticity and related variational principles, *International Journal of Solids and Structures***,** Vol.38, No.42–43, 2001, pp.7359–7380.
[8] Ahmadi, G., Linear theory of nonlocal viscoelasticity, *International Journal of Non-Linear Mechanics*, Vol.10, No.2, 1975, pp.253–258.
[9] Nowinski, J.L., On the non-local aspects of stress in a viscoelastic medium, *International Journal of Non-Linear Mechanics*, Vol.21, No.6, 1986, pp.439–446.
[10] Russell, D.L., *On mathematical models for the elastic beam with frequency-proportional damping*, In: Banks, H.T. (Ed.), Control and Estimation in Distributed Parameter Systems. SIAM, Philadelphia, PA, 125–169, 1992.
[11]Ghoneim, H., Fluid surface damping versus constrained layer damping for vibration suppression of simply supported beams, *Smart Materials and Structures*, Vol.6, No.1, 1997, pp.40–46.
[12]Lei, Y., Friswell, M.I., Adhikari, S., A Galerkin method for distributed systems with nonlocal damping, *International Journal of Solids and Structures*, Vol.43, 2006, pp.3381-3400.
[13]Munteanu, L., Chiroiu, V., Dumitriu, D., Baldovin, D., Badea, T., Chiroiu, C., On the eigenvalues optimization of Euler-Bernoulli beams with nonlocal damping pathes, *Revue Rom. Sci. Techn*., 2008 (in press).
[14]
[15] Banks, H.T., Inman, D.J., On damping mechanisms in beams, *Journal of Applied Mechanics*, Vol.58, No.3, 1991, pp.716–723.
[16] Banks, H.T., Wang, Y., Inman, D.J., Bending and shear damping in beams-frequency-domain estimation techniques, *Journal of Vibration and Acoustics*, Vol.116, No.2, 1994, pp.188–197.
[17] Sorrentino, S., Marchesiello, S., Piombo, B.A.D., A new analytical technique for vibration analysis of non-proportionally damped beams, *Journal of Sound and Vibration*, Vol.265, No.4, 2003, pp.765–782.
[18] Baldovin, D., Delsanto, P.P., Mitu, A.M., Chiroiu, V., On the modal strain energy approach, *Annual Symposium of the Institute of Solid Mechanics SISOM2007*, may 2007.
[19] Munteanu, L., Donescu, St., *Introduction to Soliton Theory: Applications to Mechanics*, Book Series "Fundamental Theories of Physics", Vol.143, Kluwer Academic Publishers, 2004.
[20] Chiroiu, V., Chiroiu, C., *Inverse problems in mechanics* (in romanian) Ed. Academiei, Bucharest,2003.
[21] Osborne, A. R., Soliton physics and the periodic inverse scattering transform, *Physica D*, Vol.86, 1995, pp.81–89.
[22] Abramowitz, M. and Stegun, I. A. (eds.), *Handbook of mathematical functions*, U. S. Dept. of Commerce, 1984.
[23] Bendsoe, M..P., Olhoff, N., Taylor, J.E., A variational formulation for multicriteria structural optimization, *Journal of Structural Mechanics*, Vol.11, No.4, 1983, pp.523-544.
[24] wseas
[25] V.Chiroiu, On the eigenvalues optimization of beams with damping patches, WSEAS Conference, Engineering Mechanics, Structures, Engineering Geology (EMESEG '09) Heraklion, Crete Island, Greece, July 22-24, 2008, ID 592-117.
[26] Munteanu, L., Delsanto, P.P., Dumitriu, D., Mosnegutu, V., ch.8, *On the characterization of auxetic matherials*, Research Trends in Mechanics, vol.2, Ed. Academiei, 2008.
[27] Chiroiu, V., Munteanu, L., Dumitriu, D., The relationship between the behavior of auxetic and negative stiffness materials. Part I. Theory, *The International Review of Mechanical Engineering* (IREME), Vol.2, No.1, 2008, pp.75-85.
[28] Chiroiu, V., Munteanu, L., Mitu, A.M., Eisinger Borcea, E., On the eigenvalues optimization of beams with auxetic patches, Annual Symposium of the Institute of Solid Mechanics SISOM2008, may 2008.
.[29] Moratti, S.C., *Materials Chem. Forum Newsletter*, 8, 2005.
[30] Love, A.E.H., *A treatise on the mathematical theory of elasticity*, 4th ed., Dover, New York 1926.
[31] Lakes, R.S., J. Materials Science, 26, 1991, pp.2287–2292.
[32] Lakes, R.S., *Physical Review Letters*, 86, 2001, pp.2897–2900.
[33] Lakes, R.S., *Philosophical Magazine Letters*, 81, 2001, pp.95–100.